

## The DAMIC-M experiment: status and first results

**I. Arnquist,<sup>a</sup> N. Avalos,<sup>b</sup> P. Bailly,<sup>c</sup> D. Baxter,<sup>d,m</sup> X. Bertou,<sup>b</sup> M. Bogdan,<sup>d</sup> C. Bourgeois,<sup>e</sup> J. Brandt,<sup>d</sup> A. Cadiou,<sup>f</sup> N. Castelló-Mor,<sup>g</sup> A.E. Chavarria,<sup>h</sup> M. Conde,<sup>h</sup> J. Cuevas-Zepeda,<sup>d</sup> A. Dastgheibi-Fard,<sup>i</sup> C. De Dominicis,<sup>c</sup> O. Deligny,<sup>e</sup> R. Desani,<sup>d</sup> M. Dhellot,<sup>c</sup> J-J. Dormard,<sup>e</sup> J. Duarte-Campderros,<sup>g</sup> E. Estrada,<sup>b</sup> N. Gadola,<sup>j</sup> R. Gaïor,<sup>c</sup> J. González Sánchez,<sup>g</sup> S. C. Hope,<sup>k</sup> T. Hossbach,<sup>a</sup> M. Huehn,<sup>h</sup> L. Iddir,<sup>c</sup> B. J. Kavanagh,<sup>g</sup> B. Kilminster,<sup>j</sup> A. Lantero-Barreda,<sup>g</sup> I. Lawson,<sup>l</sup> H. Lebbolo,<sup>c</sup> S. Lee,<sup>j</sup> P. Leray,<sup>f</sup> A. Letessier-Selvon,<sup>c</sup> P. Loaiza,<sup>e</sup> A. Lopez-Virto,<sup>g</sup> D. Martin,<sup>c</sup> K. J. McGuire,<sup>h</sup> T. Milleto,<sup>f</sup> P. Mitra,<sup>h</sup> D. Moya Martin,<sup>g</sup> S. Munagavalasa,<sup>d</sup> D. Norcini,<sup>d,k</sup> C. Overman,<sup>a</sup> S. Paul,<sup>d</sup> D. Peterson,<sup>h</sup> A. Piers,<sup>h</sup> O. Pochon,<sup>e</sup> P. Privitera,<sup>d,c,\*</sup> D. Reynet,<sup>e</sup> P. Robmann,<sup>j</sup> R. Roehnelt,<sup>h</sup> S. Scorzà,<sup>i</sup> M. Settimio,<sup>f</sup> S. A. Smee,<sup>k</sup> R. Smida,<sup>d</sup> B. Stillwell,<sup>d</sup> M. Traina,<sup>h,c</sup> P. Vallerand,<sup>e</sup> T. Van Wechel,<sup>h</sup> R. Vilar,<sup>g</sup> A. Vollhardt,<sup>j</sup> G. Warot,<sup>i</sup> D. Wolf,<sup>j</sup> R. Yajur<sup>d</sup> and J-P. Zopounidis<sup>c</sup>**

<sup>a</sup>Pacific Northwest National Laboratory (PNNL), Richland, WA, United States

<sup>b</sup>Centro Atómico Bariloche and Instituto Balseiro, Comisión Nacional de Energía Atómica (CNEA), Consejo Nacional de Investigaciones Científicas y Técnicas (CONICET), Universidad Nacional de Cuyo (UNCUYO), San Carlos de Bariloche, Argentina

<sup>c</sup>Laboratoire de physique nucléaire et des hautes énergies (LPNHE), Sorbonne Université, Université Paris Cité, CNRS/IN2P3, Paris, France

<sup>d</sup>Kavli Institute for Cosmological Physics and The Enrico Fermi Institute, The University of Chicago, Chicago, IL, United States

<sup>e</sup>CNRS/IN2P3, IJCLab, Université Paris-Saclay, Orsay, France

<sup>f</sup>SUBATECH, Nantes Université, IMT Atlantique, CNRS/IN2P3, Nantes, France

<sup>g</sup>Instituto de Física de Cantabria (IFCA), CSIC - Universidad de Cantabria, Santander, Spain

<sup>h</sup>Center for Experimental Nuclear Physics and Astrophysics, University of Washington, Seattle, WA, United States

<sup>i</sup>LPSC LSM, CNRS/IN2P3, Université Grenoble-Alpes, Grenoble, France

<sup>j</sup>Universität Zürich Physik Institut, Zürich, Switzerland

<sup>k</sup>Department of Physics and Astronomy, Johns Hopkins University, Baltimore, MD, United States

<sup>l</sup>SNOLAB, Lively, ON, Canada

<sup>m</sup>Now at Fermi National Accelerator Laboratory, Batavia, IL, United States

*E-mail:* [priviter@astro.uchicago.edu](mailto:priviter@astro.uchicago.edu)

---

\*Speaker

The DAMIC-M experiment employs thick, fully depleted silicon charge-coupled devices (CCDs) to search for sub-GeV dark matter particles. Thanks to its multiple non-destructive measurements of the pixel charge, DAMIC-M skipper CCDs achieve single-ionization charge resolution and an energy threshold in the eV-scale. We report on the progress of the experiment and first results from a prototype detector installed underground at the Laboratoire Souterrain de Modane. In particular, constraints on dark matter particles interacting with electrons are obtained in a mass range between 0.5 and 1000 MeV/c<sup>2</sup>. We also present results of a search for diurnal modulation in the measured single-ionization charge rate which significantly improves sensitivity at the lowest masses.

## 1. Introduction

The DAMIC-M (Dark Matter in CCDs at Modane) experiment searches for sub-GeV Dark Matter (DM) using skipper Charge-Coupled Devices (CCDs) under the French Alps at the Laboratoire Souterrain de Modane (LSM). DM-induced ionization events in the thick silicon bulk are detected with sub-electron resolution through non-destructive, repeated "skipper" pixel readout [1–3]. The capability of single-electron detection, combined with an extremely low dark current [4, 5], results in an energy threshold of a few eV. The completed experiment will have  $\approx 700$  g of target mass with an expected total background of a fraction of a dru<sup>1</sup>. With target exposures of kg-year, DAMIC-M will search for low mass WIMPs with sensitivity comparable to other experiments in construction [6], and explore with several orders of magnitude improvement DM candidates that arise in hidden-sector vector-portal DM theories [7, 8], with masses 1 eV–1 GeV.

Here we report on the status of DAMIC-M, which is scheduled to start operation in 2025, and first results on DM- $e^-$  interactions with prototype detectors installed in the Low-Background Chamber (LBC), a set-up supporting DAMIC-M development and already operating at LSM.

## 2. Status of DAMIC-M

The overall DAMIC-M design is shown in Fig. 1, left. The heart of the detector is an array of fifty-two CCD modules, each with four CCDs glued on a silicon carrier wafer with patterned aluminum traces (the “pitch adapter”) that carry the CCD signals (Fig. 1, right). The CCD array, protected from infrared (IR) radiation by a copper shield, is housed inside a vacuum cryostat and cooled to  $\approx 130$  K by a cryocooler. Electroformed (EF) copper [9–11] is employed for all components closest to the detector. Surrounding the cryostat is a 20-cm-thick lead shield for  $\gamma$  rays, including the inner 5 cm made from ancient Roman lead, and a 30-cm-thick high-density polyethylene neutron shield. The custom-made front-end electronics and CCD controllers are located outside the shielding. Below we highlight progress on some of the key components:

*CCDs.* The devices, designed by Lawrence Berkeley National Laboratory (Berkeley Lab) [12], are fabricated by Teledyne DALSA in Canada on  $n$ -type high-resistivity ( $>10^4 \Omega \text{ cm}$ ) silicon wafers. Each CCD is  $9 \times 2.25 \text{ cm}^2$  in size ( $6\text{k} \times 1.5\text{k} = 9 \text{ Mpixel}$ , with pixel  $15 \times 15 \mu\text{m}^2$ ) and  $670 \mu\text{m}$ -thick. It features a three-phase polysilicon gate structure with a buried p-channel, where charge carriers are collected from the fully depleted silicon bulk. To reduce cosmogenic activation of tritium, the silicon exposure to cosmic rays is minimized by using a 18-ton shielded container for transport and a 5-ton shielding for storage of the wafers at Teledyne DALSA when they are not being processed. The production is well advanced (70% completed.)

*CCD module array.* The packaging procedures of the CCD module are finalized, with protocols that minimize surface contamination and mechanical stress in the gluing of the devices and flex cable onto the pitch adapter. Extensive mechanical, thermal and electrical tests showed that the module met all design specifications. Thermal tests of a mock-CCD array showed excellent uniformity, with a maximum temperature difference of 1.5K between modules in the array.

*CCD flex cable.* Flex cables wire-bonded to the CCD modules provide the required voltage biases and clocks. Given the flex proximity to the CCD (Fig. 1, left), its radiopurity is crucial to

<sup>1</sup>1 dru = 1 event/kg/keV/day.

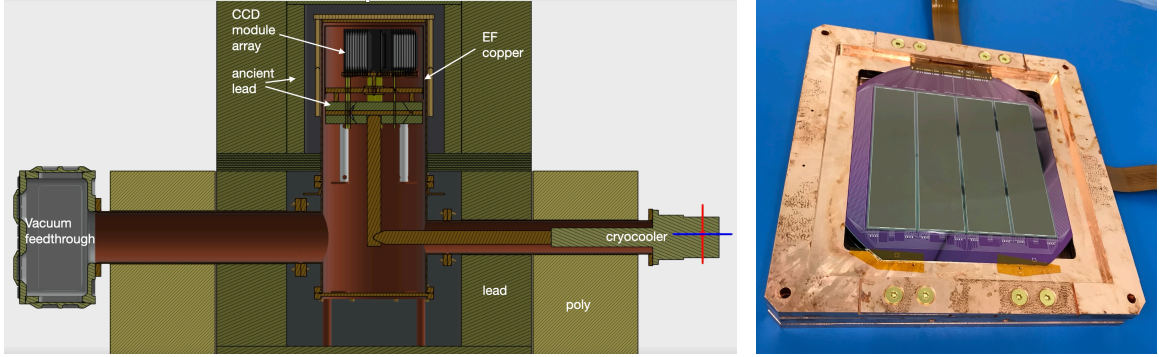


**Figure 1:** Left: Design of the DAMIC-M detector; some shielding components are not shown for clarity. Right: the CCD module in the copper box with lid removed prior to installation in the LBC.

meet the stringent radiogenic background specifications of DAMIC-M. A successful R&D with Pacific Northwest National Laboratory (PNNL) has resulted in flex cables with  $^{238}\text{U}$ ( $^{232}\text{Th}$ ) content  $\approx 100(20)$  times lower [13] than cables previously used in DAMIC at SNOLAB, a reduction sufficient for DAMIC-M purposes. The final 1.5 m-long flex, which integrates wire-bonded bare-die JFETs and silicon resistors, has been prototyped and tested, and is ready for production.

*EF copper.* Thanks to the MAJORANA collaboration, we have available high-quality EF copper for all mechanical components inside the cryostat. The copper, which was grown underground, will be machined underground at Sanford Lab, and shipped to LSM in our shielded container to minimize cosmogenic activation.

### 3. The Low-Background Chamber and First Results

The LBC (Fig. 2, left), commissioned at the LSM in early 2022, has been essential for the progress of DAMIC-M, allowing the characterization of key DAMIC-M components in a low-background environment ( $\approx 10$  dru) and a first search for DM.

The CCDs are mounted in a high-purity, oxygen-free, high-conductivity (OFHC) copper box (Fig. 1, left.), which also acts as a IR shield. To minimize leakage current, the CCDs are operated at low temperature ( $\approx 130$  K) under vacuum (pressure  $\sim 5 \times 10^{-6}$  mbar) inside the LBC cryostat. The CCD box is surrounded by at least 7.5 cm of very low-background lead ( $\leq 7$  mBq/kg  $^{210}\text{Pb}$ ), with the innermost 2 cm of ancient origin, to mitigate gamma radiation from components located in the cryostat. In addition, 15 cm of low-background lead (54 Bq/kg  $^{210}\text{Pb}$ ) and 20 cm of high-density polyethylene surround the cryostat to attenuate high-energy  $\gamma$ -rays and neutrons. All parts of the detector are appropriately cleaned to remove any surface contamination [14, 15]. Voltage biases and clocks to operate the devices are provided by a commercial CCD controller placed outside the external shielding. A Slow Control system enables the remotely controlled operation of the LBC.

A background of  $\sim 10$  dru was measured during the initial operation of the LBC, similar to that of DAMIC at SNOLAB [16]. This level of background matches a full simulation of the apparatus with GEANT4 [17], which includes realistic amounts of radioactive contaminants as determined by radioassay measurements and bookkeeping of cosmogenic activation time of materials.

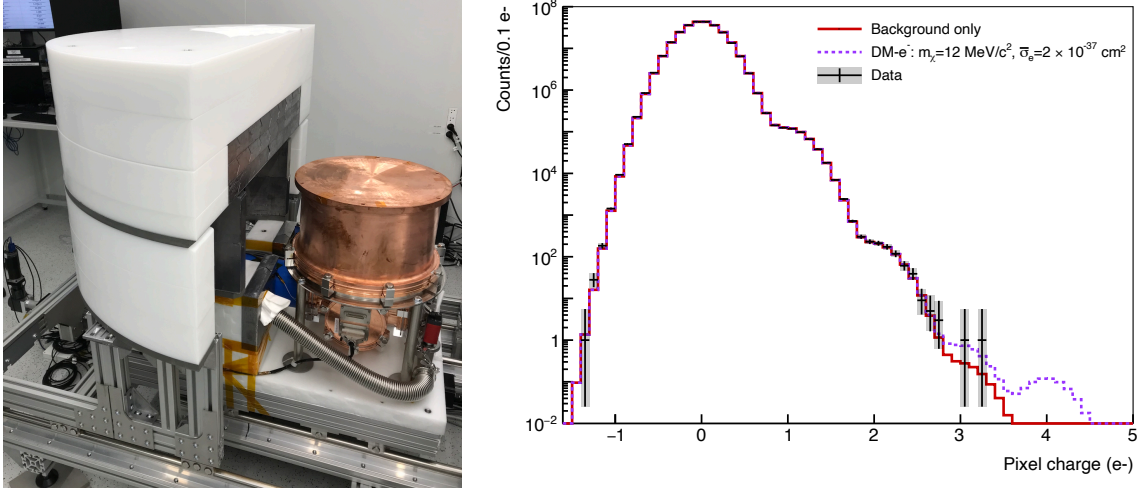


**Figure 2:** Left: The Low Background Chamber at the LSM, outside the movable shielding (half of it visible.) Right: Pixel charge distribution with peaks corresponding to individual charges. The red line is the fit result for the background-only hypothesis (no DM- $e^-$ ). The dashed violet line is the expectation for background plus a DM- $e^-$  heavy-mediator model with  $m_\chi=12\text{ MeV}/c^2$  and cross section equal to our 90% CL limit value obtained at this mass.

DAMIC-M skipper CCDs, from first prototypes to the CCD module, were characterized in the LBC. Different operating parameters (clock/bias voltage levels and clock timing widths) were evaluated to reduce clock-induced charge and optimize charge transfer. Temperature scans were performed to characterize the temperature dependence of dark current. CCDs were exposed to ionizing radiation to study its effect on dark current [18].

In 2022, we collected data in stable conditions with prototype skipper CCDs (6k×4k pixel) to perform a first search for DM- $e^-$  interactions. In this early LBC commissioning phase, the dark current ( $\approx 20\text{ e}^-/\text{mm}^2/\text{day}$ ) was several times higher than the lowest reached in CCDs [4, 5], but sufficiently low to perform a sensitive search for DM.

CCD images are first calibrated from the fitted position of the  $0e^-$  and  $1e^-$  peaks in the pixel charge distribution (Fig. 2, right). Then contiguous pixels with charge are joined into clusters. Those with total charge  $>7e^-$  are excluded from further analysis since they are unlikely to be produced by sub-GeV DM- $e^-$  interactions. For each cluster we also exclude several trailing pixels in the horizontal and vertical directions to account for charge transfer inefficiencies. Defects in the CCDs may release charge during the readout, appearing in the images as “hot” pixels and columns [19]. These are identified by their increased rate of pixels with  $1e^-$ , and rejected. Lastly, we exclude portions of the CCD with charge traps in the serial register (identified by a decreased rate of pixels with  $1e^-$ ). After applying the selection criteria  $3.68 \times 10^8$  pixels remain, corresponding to an integrated exposure of 85.23 g-days. No pixel with charge  $\geq 4e^-$  and  $\leq 7e^-$  is found, improving by one order of magnitude previous limits in silicon at these charge multiplicities [5]. We then fit the pixel charge spectrum (Fig. 2, right) as the sum of the expected DM- $e^-$  scattering signal and the background model (Poisson dark current.) Details are in Ref. [20].

In Ref. [21] we introduce a new method to constrain DM- $e^-$  scattering, which exploits a daily

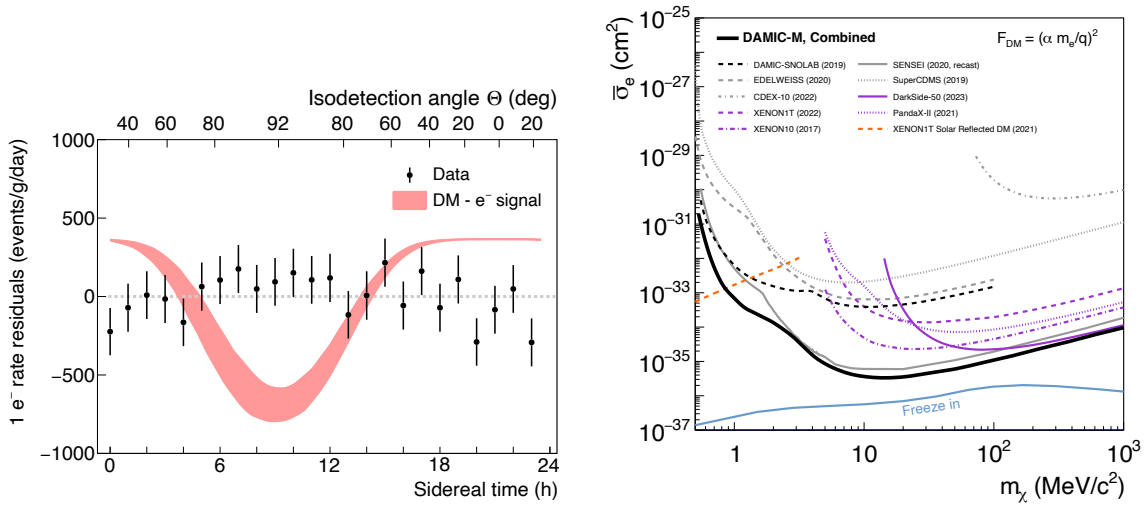


**Figure 3:** Left: Residual  $1e^-$  rate after the subtraction of the background model, as a function of local apparent sidereal time. The light red band shows the expected daily-modulated signal for a DM particle of mass  $1 \text{ MeV}/c^2$ ,  $\bar{\sigma}_e = 10^{-32} \text{ cm}^2$  interacting via an ultralight dark photon mediator. Right: DAMIC-M 90% C.L. upper limits (solid thick black) on DM- $e^-$  interactions through an ultralight mediator obtained combining results from Refs. [20, 21].

modulation of the DM signals. In fact, the velocity distribution of DM particles at the detector may be distorted by their interactions in the Earth [22–24]. Over the course of a sidereal day, the position of the detector rotates with respect to the incoming DM flux. Thus, the DM particles will travel a greater or smaller distance across the Earth at different times, leading to a daily modulation. We search for a daily modulation of the measured rate of  $1e^-$  pixels (Fig. 3, left) in a portion of the data (39.97 g-days), corresponding to 63 days of uninterrupted data taking with images acquired every  $\approx 10$  min. This search is sensitive for DM masses  $\leq 2.7 \text{ MeV}/c^2$ .

In both analyses no preference is found for a DM signal at any mass and constraints are derived accordingly. The 90% C.L. exclusion limit for an ultralight mediator combining the two results is shown in Fig. 3, right. Notably, the daily modulation search improve the limits reported in Ref. [20] by up to two orders of magnitude for DM mass  $\leq 2.7 \text{ MeV}/c^2$ .

#### 4. Outlook

The design of DAMIC-M is complete, and the detector is in its construction phase with start of operation scheduled in 2025. We will continue to operate the LBC to support the DAMIC-M program, with several upgrades and measurement campaigns foreseen. We recently replaced the OFHC copper lids of the LBC CCD box with EF copper ones (fabricated by the Canfrac Underground Laboratory facilities), which reduced the background from  $\sim 10$  to  $\sim 5$  dru. LBC data taking is ongoing, currently focused on background measurements (including  $^{32}\text{Si}$  in CCDs made from the same ingot of the DAMIC-M production), and we will upgrade the set-up with the final DAMIC-M electronics in early 2024. We plan to collect few months of DM search data with optimal conditions for dark current and noise to reach 1 kg-day of exposure, which will provide a tenfold improvement over our current limits before the start of DAMIC-M installation.

## Acknowledgments

We thank the LSM for their support in the installation and operation of the detector underground. The DAMIC-M project has received funding from the European Research Council (ERC) under the European Union’s Horizon 2020 research and innovation programme Grant Agreement No. 788137, and from NSF through Grant No. NSF PHY-1812654. The work at University of Chicago and University of Washington was supported through Grant No. NSF PHY-2110585. This work was supported by the Kavli Institute for Cosmological Physics at the University of Chicago through an endowment from the Kavli Foundation. We thank the College of Arts and Sciences at University of Washington for contributing the first CCDs to the DAMIC-M project. IFCA was supported by project PID2019-109829GB-I00 funded by MCIN/ AEI /10.13039/501100011033. BJK acknowledges funding from the Ramón y Cajal Grant RYC2021-034757-I, financed by MCIN/AEI/10.13039/501100011033 and by the European Union “NextGenerationEU”/PRTR. The Centro Atómico Bariloche group is supported by ANPCyT grant PICT-2018-03069. The University of Zürich was supported by the Swiss National Science Foundation. The CCD development work at Lawrence Berkeley National Laboratory MicroSystems Lab was supported in part by the Director, Office of Science, of the U.S. Department of Energy under Contract No. DE-AC02-05CH11231. We thank Teledyne DALSA Semiconductor for CCD fabrication. We acknowledge Santander Supercomputing support group at the University of Cantabria who provided access to the supercomputer Altamira at the Institute of Physics of Cantabria (IFCA-CSIC), member of the Spanish Supercomputing Network, for performing simulations.

## References

- [1] J. Janesick, T. Elliott, A. Dingiziam, R. Bredthauer, C. Chandler, J. Westphal et al., *New advancements in charge-coupled device technology: subelectron noise and 4096 x 4096 pixel CCDs*, *Proc. SPIE* **1242** (1990) 223.
- [2] J. Tiffenberg, M. Sofo-Haro, A. Drlica-Wagner, R. Essig, Y. Guardincerri, S. Holland et al., *Single-electron and single-photon sensitivity with a silicon Skipper CCD*, *Phys. Rev. Lett.* **119** (2017) 131802.
- [3] DAMIC-M COLLABORATION collaboration, *Precision measurement of Compton scattering in silicon with a skipper CCD for dark matter detection*, *Phys. Rev. D* **106** (2022) 092001.
- [4] DAMIC COLLABORATION collaboration, *Constraints on Light Dark Matter Particles Interacting with Electrons from DAMIC at SNOLAB*, *Phys. Rev. Lett.* **123** (2019) 181802.
- [5] SENSEI COLLABORATION collaboration, *SENSEI: Direct-Detection Results on sub-GeV Dark Matter from a New Skipper-CCD*, *Phys. Rev. Lett.* **125** (2020) 171802 [2004.11378].
- [6] SUPERCDMS COLLABORATION collaboration, *Projected Sensitivity of the SuperCDMS SNOLAB experiment*, *Phys. Rev. D* **95** (2017) 082002.
- [7] C. Boehm and P. Fayet, *Scalar dark matter candidates*, *Nucl. Phys.* **B683** (2004) 219.

[8] X. Chu, T. Hambye and M. Tytgat, *The Four Basic Ways of Creating Dark Matter Through a Portal*, *J. Cosmol. Astropart. Phys.* **1205** (2012) 034.

[9] E. Hoppe, C. Aalseth, O. Farmer, T. Hossbach, M. Liezers, H. Miley et al., *Reduction of radioactive backgrounds in electroformed copper for ultra-sensitive radiation detectors*, *Nucl. Instrum. Meth. A* **764** (2014) 116.

[10] B. LaFerriere, T. Maiti, I. Arnquist and E. Hoppe, *A novel assay method for the trace determination of Th and U in copper and lead using inductively coupled plasma mass spectrometry*, *Nucl. Instrum. Meth. A* **775** (2015) 93.

[11] S. Borjabad, J.C. Amaré, I.C. Bandac, M.L. di Vacri, A. Ianni and S. Nisi, *Copper electroforming service at Laboratorio Subterráneo de Canfranc*, *AIP Conference Proceedings* **1921** (2018) 020001  
[\[https://pubs.aip.org/aip/acp/article-pdf/doi/10.1063/1.5018987/14007591/020001\\_1\\_online.pdf\]](https://pubs.aip.org/aip/acp/article-pdf/doi/10.1063/1.5018987/14007591/020001_1_online.pdf)

[12] S. Holland, D. Groom, N. Palaio, R. Stover and M. Wei, *Fully depleted, back-illuminated charge-coupled devices fabricated on high-resistivity silicon*, *IEEE Trans. Electron Devices* **50** (2003) 225.

[13] I.J. Arnquist, M.L. di Vacri, N. Rocco, R. Saldanha, T. Schlieder, R. Patel et al., *Ultra-low radioactivity flexible printed cables*, *EPJ Tech. Instrum.* **10** (2023) 17 [2303.10862].

[14] E. Hoppe, A. Seifert, C. Aalseth, P. Bachelor, A. Day, D. Edwards et al., *Cleaning and passivation of copper surfaces to remove surface radioactivity and prevent oxide formation*, *Nucl. Instrum. Meth. A* **579** (2007) 486.

[15] N. Abgrall et al., *The Majorana Demonstrator radioassay program*, *Nuclear Instruments and Methods in Physics Research Section A: Accelerators, Spectrometers, Detectors and Associated Equipment* **828** (2016) 22.

[16] DAMIC COLLABORATION collaboration, *Characterization of the background spectrum in DAMIC at SNOLAB*, *Phys. Rev. D* **105** (2022) 062003.

[17] S. Agostinelli et al., *Geant4 — a simulation toolkit*, *Nuclear Instruments and Methods in Physics Research Section A: Accelerators, Spectrometers, Detectors and Associated Equipment* **506** (2003) 250.

[18] R.S. for the DAMIC-M Collaboration, *Damic-m: Background and dark current studies with low background chamber*, EXCESS23@TAUP Workshop (Vienna, 2023),  
<https://indico.cern.ch/event/1213348/contributions/5411352/>.

[19] J. Janesick, *Scientific Charge-Coupled Devices*, Press Monographs, The International Society for Optical Engineering, Bellingham, WA (2001).

[20] DAMIC-M COLLABORATION collaboration, *First Constraints from DAMIC-M on Sub-GeV Dark-Matter Particles Interacting with Electrons*, *Phys. Rev. Lett.* **130** (2023) 171003 [2302.02372].

- [21] I. Arnquist, N. Avalos, D. Baxter, X. Bertou, N. Castello-Mor, A.E. Chavarria et al., *Search for daily modulation of mev dark matter signals with damic-m*, 2023.
- [22] J.I. Collar and F.T. Avignone, *Diurnal modulation effects in cold dark matter experiments*, *Phys. Lett. B* **275** (1992) 181.
- [23] J.I. Collar and F.T. Avignone, III, *The Effect of elastic scattering in the Earth on cold dark matter experiments*, *Phys. Rev. D* **47** (1993) 5238.
- [24] F. Hasenbalg, D. Abriola, F.T. Avignone, J.I. Collar, D.E. Di Gregorio, A.O. Gattone et al., *Cold dark matter identification: Diurnal modulation revisited*, *Phys. Rev. D* **55** (1997) 7350 [[astro-ph/9702165](#)].